

Doping-induced perturbation and percolation in the two-dimensional Anderson lattice

Lan-ying Wei^{1,2} and Yi-feng Yang^{1,2,3,*}

¹Beijing National Laboratory for Condensed Matter Physics and Institute of Physics, Chinese Academy of Sciences, Beijing 100190, China

²School of Physical Sciences, University of Chinese Academy of Sciences, Beijing 100190, China

³Collaborative Innovation Center of Quantum Matter, Beijing 100190, China

*yifeng@iphy.ac.cn

ABSTRACT

We examine the doping effects in the two-dimensional periodic Anderson model using the determinant Quantum Monte Carlo (DQMC) method. We observe bound states around the Kondo hole site and find that the heavy electron states are destroyed at the nearest-neighbor sites. Our results show no clear sign of hybridization oscillation predicted in previous mean-field calculations. We further study the electron transport with increasing doping and as a function of temperature and obtain a critical doping $x_c \approx 0.6$ that marks a transition from the Kondo insulator regime to the single-ion Kondo regime. The value of x_c is in good agreement with the predicted threshold for the site percolation. Our results confirm the percolative nature of the insulator-metal transition widely observed in doped Kondo insulators.

Introduction

Chemical substitution or doping of the magnetic ions (Ce, Yb, U, ...) by its nonmagnetic counterpart element (La, Th, Y, ...) gives rise to local vacancies of the magnetic f -moments (called the Kondo holes) and could cause dramatic changes in the ground state properties of heavy fermion compounds. In Kondo insulators such as CeNiSn¹⁻³, CeRhSb^{2,3}, and Ce₃Bi₄Pt₃⁴, interesting new physics has been proposed such as the bound states near the Kondo holes⁵⁻⁹. With increasing concentrations of doping, an insulator-to-metal transition has been widely observed, accompanying with the change from the dense Kondo lattice regime to the single-ion Kondo regime. This transition has been generally speculated to be of percolative nature¹⁰. Many work, mostly based on mean-field calculations, have been carried out in order to clarify the relevant physics^{7,11}. To the best of our knowledge, no exact numerical calculations has been done. In particular, it is not clear how Kondo holes may destroy the many-body heavy electron state and, with increasing doping, drive the system from the Kondo lattice physics to the single-ion Kondo physics.

In this work, we use the determinant Quantum Monte Carlo (DQMC) method to study the electronic and transport properties of the doped two-dimensional periodic Anderson lattice. DQMC is an exact numerical method for a finite lattice but often suffers from severe sign problem away from the half filling. We therefore focus on the vicinity of the half filling case and study the doping effect in a Kondo insulator simply by tuning the energy levels of a selected number of local f -electron sites. For sufficiently depleted (or doubly occupied) local f -levels, this is equivalent to replace the local magnetic ions by the nonmagnetic counterparts. We find no severe sign problem in the considered temperature and tuning range. This allows us to study the evolution of the electronic states with arbitrary number of Kondo holes. We are able to reproduce the predicted bound states around the Kondo hole site obtained in previous mean-field calculations and find that the hybridized heavy electron states are destroyed in the nearest-neighbor sites. We further study the electronic transport with increasing doping and confirm the percolation transition from the Kondo insulator state in the dense Kondo lattice to the single-ion Kondo behavior in the diluted limit.

Results

We start with the following modified Hamiltonian for the periodic Anderson lattice,

$$H = -t \sum_{\langle ij \rangle, \sigma} (c_{i\sigma}^\dagger c_{j\sigma} + \text{H.c.}) + V \sum_{i, \sigma} (c_{i\sigma}^\dagger f_{i\sigma} + \text{H.c.}) + U \sum_i (n_{i\uparrow}^f - \frac{1}{2})(n_{i\downarrow}^f - \frac{1}{2}) + \sum_{l, \sigma} \epsilon_l^f f_{l\sigma}^\dagger f_{l\sigma}, \quad (1)$$

where $c_{i\sigma}^\dagger$ ($f_{i\sigma}^\dagger$) and $c_{i\sigma}$ ($f_{i\sigma}$) are the creation and annihilation operators for the conduction and f -electrons, respectively. $n_{i\sigma}^c = c_{i\sigma}^\dagger c_{i\sigma}$ and $n_{i\sigma}^f = f_{i\sigma}^\dagger f_{i\sigma}$ are the corresponding number operators for the spin- σ component on the i -th site, t is the

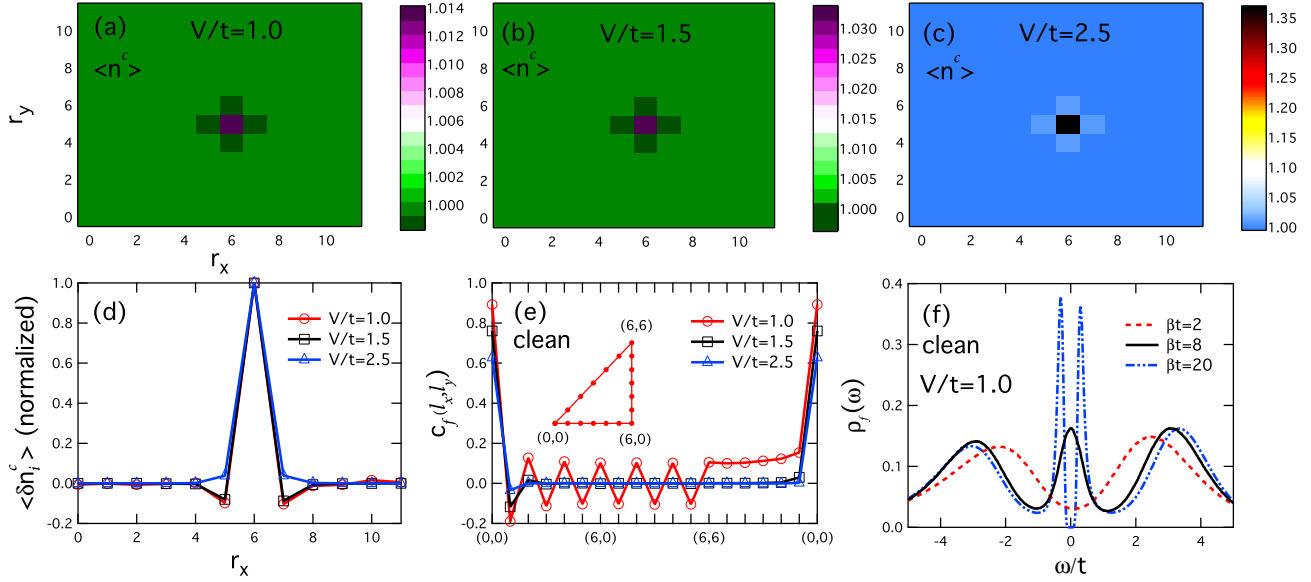


Figure 1. Perturbation of a single Kondo hole to the charge density of the conduction electrons. (a-c) Contour plots of the occupation number of the conduction electrons, $\langle n^c \rangle$, with a single Kondo hole for $V/t=1.0$, 1.5 and 2.5, respectively. (d) The perturbation, $\langle \delta n_i^c \rangle - 1.0$, along r_x across the Kondo hole site as shown in (a-c). (e) The spin correlation function $c_f(l_x, l_y)$ of the f -electrons in the clean lattice along a triangular path shown in the inset. (f) The local density of states of the f -electrons in the clean lattice for $V/t=1.0$ with varying temperature. Other parameters are $\beta t = 20$ in (a-e) and $\epsilon_f^I/t = 30$ in (a-d).

hopping parameter of the conduction electrons between the nearest-neighbor sites, V describes the local hybridization between the conduction and f -electrons, and U is the local Coulomb interaction on the local f -site. ϵ_f^I represents the f -electron energy at the impurity sites I , which is tuned away from zero to resemble the effect of chemical substitution. The sum \sum^I in the last term is only over the impurity sites. We have modified the DQMC code implemented in QUANTUM Electron Simulation Toolbox¹² for the tuning and carried out numerical simulations on a 12×12 square lattice with a discretization of the imaginary time, $\Delta\tau = 0.25$. For $\epsilon_f^I = 0$, the model reduces to a clean Kondo lattice, which has no sign problem due to the particle-hole symmetry. For large $|\epsilon_f^I|$, the local f -electron occupation is effectively empty or full, so the f -electron degree of freedom at the impurity site plays essentially no role in the simulation and we also find no severe sign problem. The magnetic and electronic properties of the f -electrons can be obtained through the equal-time spin correlation function^{13,14},

$$c_f(l_x, l_y) = \frac{1}{N} (-1)^{l_x + l_y} \langle (n_{i+l\uparrow}^f - n_{i+l\downarrow}^f) (n_{i\uparrow}^f - n_{i\downarrow}^f) \rangle, \quad (2)$$

and the imaginary time Green's function,

$$G_{f;i\sigma}(\tau) = \langle T_\tau f_{i\sigma}(\tau) f_{i\sigma}^\dagger(0) \rangle. \quad (3)$$

The local density of states of the f -electrons, $\rho_{f;i\sigma}(\omega)$, can be obtained from $G_{f;i\sigma}(\tau)$ using the maximum entropy method,

$$G_{f;i\sigma}(\tau) = \int_{-\infty}^{\infty} d\omega \frac{e^{-\omega\tau}}{1 + e^{-\beta\omega}} \rho_{f;i\sigma}(\omega). \quad (4)$$

The same can be done for the conduction electrons. For simplicity, we set $t = 1$ and $U/t = 6$ in the numerical calculations and use the natural units with the Boltzmann constant $k_B = 1$. The large value of U is chosen for typical Kondo lattice systems^{15,16}.

To provide a basis for comparison, we first present the results for the clean lattice ($\epsilon_f^I = 0$) in Figs. 1(e) and 1(f). The spin correlation function at low temperature ($T/t = 0.05$) exhibits clear antiferromagnetic spatial oscillation for $V/t = 1.0$, indicating antiferromagnetic long-range order in the finite lattice for weak hybridization. For stronger hybridization with $V/t = 1.5$ and 2.5, the antiferromagnetic oscillation is suppressed and, as expected, the system shows a transition from the antiferromagnetically long-range ordered state to the paramagnetic (disordered) state with increasing hybridization due to the competition between the collective Kondo hybridization and the induced RKKY (Ruderman-Kittel-Kasuya-Yosida) exchange

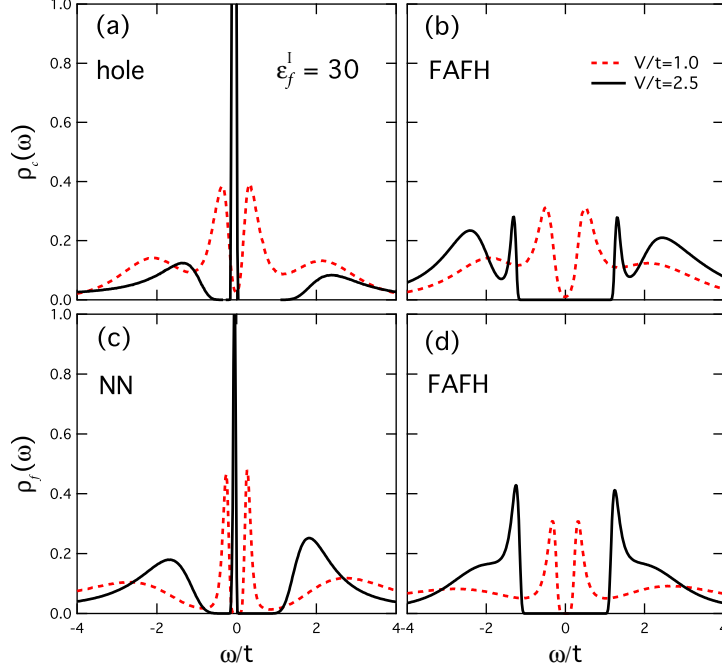


Figure 2. Bound states in the local densities of states around the Kondo hole. (a,b) The local density of states $\rho_c(\omega)$ of the conduction electrons at the Kondo hole site and far away from hole (FAFH) site. (c,d) The local density of states $\rho_f(\omega)$ of the f -electrons at the nearest-neighbor (NN) site and far away from hole (FAFH) site for different hybridization strengths $V/t = 1.0$ and 2.5 . Other parameters are $\epsilon_f^I/t = 30$ and $\beta t = 20$.

coupling among the f -moments¹⁷. Fig. 1(f) plots the f -electron local density of states at $V/t = 1.0$. We see for $T/t = 0.5$ two broad Hubbard peaks located at $\omega = \pm U/2 = \pm 3$. As temperature decreases, a narrow resonance peak first appears at $T/t = 0.125$, reflecting the onset of coherence, and then splits into two sharp peaks at $T/t = 0.05$. The split of the resonance peak is a special feature of the Anderson lattice model and originates from the collective hybridization between the conduction band and the effective f -electron flat band near the Fermi energy. The emergence of the gap feature indicates that collective hybridization already takes place in the antiferromagnetic state.

The effect of doping can be readily obtained by comparing the results for the clean Anderson lattice ($\epsilon_f^I = 0$) and that with a finite ϵ_f^I . Figs. 1(a-d) plot the spatial distribution of the average $\langle n_{i\sigma}^c \rangle$, the occupation number of the conduction electrons, for $\epsilon_f^I/t = 30 \gg D = 4t = 4$. This resembles the situation of a Kondo hole, as the local f -electron occupation number at the impurity site is almost zero. On the other hand, the local occupation of the conduction electrons, $\langle n_{i\sigma}^c \rangle$, is strongly enhanced and increases rapidly with increasing V . This may be understood if we integrate out the local f -electron degree of freedom at the impurity site. We obtain effectively a local attractive potential, $\delta\epsilon_c^I \propto -V^2/|\epsilon_f^I|$, which tends to trap the conduction electrons on the Kondo hole site, causing the increase of $\langle n_{i\sigma}^c \rangle$. For small $V/t = 1.0$ and 1.5 , we see that $\langle n_{i\sigma}^c \rangle$ is enhanced at the impurity site while slightly reduced in the nearest-neighbor sites. The charge density oscillation is also associated with this potential scattering, reflecting the effect of Friedel oscillation of free conduction electrons. This is possible because for sufficiently small V , the scattering potential is relatively stronger and overcomes the hybridization energy, $\Delta_h \propto D e^{-aUt/V^2}$, where a is a constant of the order of unity. As expected, there is no oscillation for strong hybridization at $V/t=2.5$. $\langle n_{i\sigma}^c \rangle$ exhibits a rapid decay with increasing distance away from the Kondo hole. We note that unlike previous mean-field studies¹⁸⁻²⁰, we observe no evident spatial oscillation in the hybridization function²¹, indicating that the perturbation is suppressed in our model, possibly due to the half filling.

The perturbation to the local electronic densities of states is presented in Fig. 2 and compared with that far away from the Kondo hole site (FAFH) for $V/t = 1.0$ and 2.5 . The latter is the same as that in the clean lattice. As shown in Figs. 2(a) and 2(c), a sharp peak emerges inside the hybridization gap for both ρ_c at the Kondo hole site and ρ_f at the nearest-neighbor sites for $V/t = 2.5$, in contrast to the unperturbed results far away from the Kondo hole site. The resonance peak gives the well-known bound states and is missing if hybridization strength at the hole site is set to zero (no impurity scattering). For small V , the bound states are absent due to weak impurity scattering as discussed above and the peaks at the edges of the hybridization gap reflect the hybridization between the conduction electrons and the f -moments, similar to those in the clean

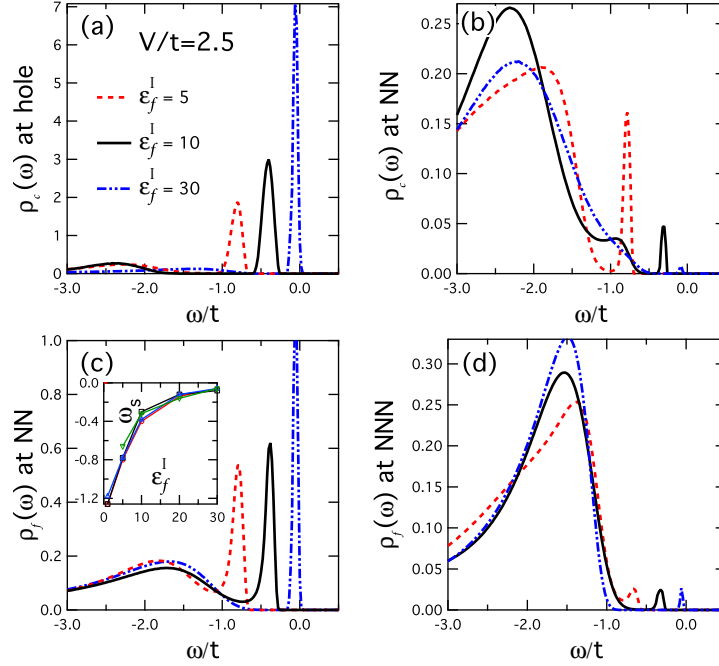


Figure 3. The variation of the bound states with ε_f^I . (a,b) The local density of states $\rho_c(\omega)$ of the conduction electrons at the impurity site and the nearest-neighbor (NN) site. (c,d) The local density of states, $\rho_f(\omega)$, of the f -electrons at the nearest-neighbor (NN) site and the next-nearest-neighbor (NNN) site. The impurity level is taken to be $\varepsilon_f^I/t = 5, 10, 30$. The inset in (c) shows the location ω_s of the bound state as a function of ε_f^I . Other parameters are $V/t = 2.5$ and $\beta t = 20$.

lattice. The suppression of these hybridization states at the gap edges for $V/t = 2.5$ is a manifestation of the destruction of the heavy electrons due to the presence of the nearby Kondo hole. This suggests that the heavy electron emergence is not a single-site property but a collective phenomenon that involves correlations among neighboring sites in the dense Kondo lattice.

Fig. 3 further compares the densities of states at different sites and for varying ε_f^I . We see that the height of the resonance peak is reduced substantially by over an order of magnitude further away from the impurity site. Nevertheless, as ε_f^I increases, the bound states move uniformly towards the center of the hybridization gap and become more and more pronounced. The change in their location is shown as a function of ε_f^I in the inset of Fig. 3(c). We obtain similar curves for the peaks in both ρ_c at the hole site and ρ_f at the NN sites, indicating their common origin. As expected, the bound state approaches $\omega = 0$ as $\varepsilon_f^I \rightarrow \infty$, consistent with the mean-field prediction.

Next, we study how increasing doping may change the electronic and transport properties by tuning the system from the Kondo insulator to the diluted limit. We add more impurity sites whose positions are chosen randomly in the numerical simulation and calculate the dc conductivity of the doped Anderson lattice using the approximation,

$$\sigma_{dc} = \frac{\beta^2}{\pi} g_{xx}(\tau = \beta/2), \quad (5)$$

in which $g_{xx}(\tau)$ is the current-current correlation function in imaginary time,

$$g_{xx}(\tau) = -\langle T_\tau j_x(\tau) j_x(0) \rangle, \quad (6)$$

with

$$j_x(\tau) = it \sum_{l\sigma} \left[c_{l+x,\sigma}^\dagger(\tau) c_{l,\sigma}(\tau) - c_{l,\sigma}^\dagger(\tau) c_{l+x,\sigma}(\tau) \right]. \quad (7)$$

The resulting conductivity, σ_{dc} , is plotted in Fig. 4 as a function of doping x for different temperatures. The data presented here are an average over only 5 samples of random configurations. We have checked the results up to 20 samples and found a numerical error of less than 5%. We see all curves cross at a critical doping, $x_c \approx 0.6$, indicating opposite temperature

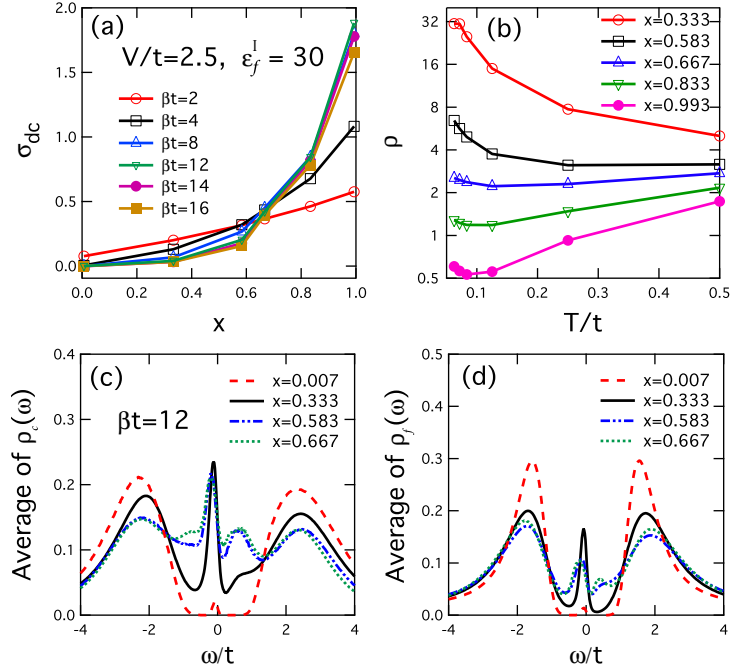


Figure 4. Percolation transition from the Kondo insulator state to the single-ion Kondo state with increasing doping. (a) The dc conductivity σ_{dc} as a function of doping x at different temperatures. (b) The resistivity $\rho = 1/\sigma_{dc}$ as a function of temperature for various doping x . (c,d) The average $\rho_c(\omega)$ and $\rho_f(\omega)$ at $\beta t = 12$ for different x . Other parameters are $V/t = 2.5$ and $\epsilon_f^I/t = 30$.

dependence below and above x_c . Moreover, our analysis of finite size effect shows no significant change in x_c with increasing L (see Supplementary Fig. S1). For $x < 0.6$, σ_{dc} is small and the resistivity, $\rho = 1/\sigma_{dc}$, increases as temperature decreases, so that the system is in the Kondo insulator phase. As x becomes larger than 0.6, σ_{dc} increases rapidly with x as the system approaches the single-ion Kondo limit. In this regime, $\rho(T)$ first decreases with decreasing temperature and exhibits metallic behavior at high temperatures down to about $T < 0.1$, below which the resistivity becomes insulating like, with a minimum signalling the typical single-ion Kondo behavior in the diluted limit. Our calculations therefore cover the whole doping range from the dense Kondo lattice to the single-ion Kondo limit.

To understand the connection between the transport property and the bound states, we calculate the average densities of states of both the conduction and f -electrons on all sites. The results are plotted in Figs. 4(c) and 4(d). We see that the average impurity states exhibit broad peaks inside the hybridization gap, similar to the mean-field results. For $x = 0.333, 0.583$ and 0.667 , the gap is gradually filled in, yielding a finite density of states at $\omega = 0$, in contrast to the insulating like behavior shown in our calculated resistivity curve. Hence the average density of states cannot be used directly to explain the transport properties. This points to the percolative nature of the electron transport. In the theory of site percolation¹⁰, adjacent bound states could form a cluster. When the size of the cluster grows and eventually percolates through the whole lattice after stochastic doping of enough sites, the system reaches a percolation threshold where a phase transition takes place. For the square lattice of infinite size in two dimension with only nearest-neighbor hopping, the percolation threshold is $x_c \approx 0.593$ ¹⁰. Increasing the number of coordination or dimension can reduce the threshold⁹. In our two dimensional 12×12 system, bound states are only pronounced at the hole site for the conduction electrons. Since only nearest-neighbor hopping is allowed, the impurity sites have to be connected to form a network in order for the conduction electrons to move from one side to the other side of the lattice. As shown in Fig. 4, the critical doping $x_c \approx 0.6$ obtained in our resistivity calculations is in good agreement with the percolation threshold x_c . Moreover, previous theories have also predicted for $T = 0$ and $x > x_c$ a power law scaling, $\sigma_{dc} \propto (x - x_c)^\mu$, with $\mu \approx 1.3$ ²², consistent with our fit giving $\mu \approx 1.44$ for $L = 12$ and $\beta t = 16$ (see Supplementary Fig. S2). The doping-induced insulator-metal transition is therefore an indication of site percolation of the conducting electrons through the bound states, which governs the charge transport in the heavily doped Kondo lattice. Our results confirm the previous theoretical and experimental speculations. Along the percolation path, collective hybridizations are destroyed around the impurity sites, providing an explanation to the crossover from the heavy electron physics to the single-ion Kondo physics.

Conclusion

We use the determinant Quantum Monte Carlo (DQMC) method to study the doping effects in the two-dimensional periodic Anderson lattice. We observe the suppression of the hybridization feature in the vicinity of the Kondo hole, which suggests a physical mechanism to destroy the heavy electron states with increasing doping. Our results also confirm the bound states appearing around the Kondo hole, but show no obvious signature of the hybridization oscillation predicted in the mean-field calculations. We further study the evolution of the electron transport with increasing doping and demonstrate the percolative nature of the insulator-metal transition from the dense Kondo lattice to the single-ion Kondo limit. We obtain a critical doping that is consistent with the predicted threshold for site percolation.

References

1. Echizen, Y. & Takabatake, T. Effect of Kondo-hole impurity on the pseudogap in CeNiSn. *Physica B: Condens. Mat.* **259**, 292–293 (1999).
2. Adroja, D. T., Rainford, B. D., Neville, A. J., Mandal, P. & Jansen, A. G. M. A comparative study of suppression of the energy gap with La substitution in the Kondo insulators: CeNiSn and CeRhSb. *J. Magn. Magn. Mater.* **161**, 157–168 (1996).
3. Goraus, J. & Ślebarski, A. Quantum critical transition from Kondo insulator to metallic state studied by band-structure calculations for doped compounds: CeRhSb and CeNiSn. *Phys. Status Solidi B* **250**, 533–536 (2013).
4. Pietrus, T., Löhneysen, H. v. & Schlottmann, P. Kondo-hole conduction in the La-doped Kondo insulator Ce₃Bi₄Pt₃. *Phys. Rev. B* **77**, 115134 (2008).
5. Sollie, R. & Schlottmann, P. A simple theory of the Kondo hole. *J. Appl. Phys.* **69**, 5478–5480 (1991).
6. Sollie, R. & Schlottmann, P. Local density of states in the vicinity of a Kondo hole. *J. Appl. Phys.* **70**, 5803–5805 (1991).
7. Schlottmann, P. Impurity bands in Kondo insulators. *Phys. Rev. B* **46**, 998–1004 (1992).
8. Schlottmann, P. Influence of a Kondo-hole impurity band on magnetic instabilities in Kondo insulators. *Phys. Rev. B* **54**, 12324–12331 (1996).
9. Schlottmann, P. & Hellberg, C. S. Metal-insulator transition in dirty Kondo insulators. *J. Appl. Phys.* **79**, 6414–6416 (1996).
10. Aharony, A. & Stauffer, D. *Introduction to percolation theory* (Taylor & Francis, 2003).
11. Li, Z.-z., Xu, W., Chen, C. & Xiao, M.-w. Alloying effects of Kondo insulators. *Phys. Rev. B* **50**, 11332–11339 (1994).
12. Tomas, A., Chang, C.-C., Scalettar, R. & Bai, Z. Advancing large scale many-body QMC simulations on GPU accelerated multicore systems. In *Parallel & Distributed Processing Symposium (IPDPS), 2012 IEEE 26th International*, 308–319 (IEEE, 2012).
13. Hirsch, J. E. & Tang, S. Antiferromagnetism in the two-dimensional Hubbard model. *Phys. Rev. Lett.* **62**, 591–594 (1989).
14. Vekić, M., Cannon, J. W., Scalapino, D. J., Scalettar, R. T. & Sugar, R. L. Competition between antiferromagnetic order and spin-liquid behavior in the two-dimensional periodic Anderson model at half filling. *Phys. Rev. Lett.* **74**, 2367–2370 (1995).
15. Jiang, M., Curro, N. J. & Scalettar, R. T. Universal knight shift anomaly in the periodic anderson model. *Phys. Rev. B* **90**, 241109 (2014).
16. Shim, J., Haule, K. & Kotliar, G. Modeling the localized-to-itinerant electronic transition in the heavy fermion system CeIrIn₅. *Science* **318**, 1615–1617 (2007).
17. Doniach, S. The Kondo lattice and weak antiferromagnetism. *Physica B+C* **91**, 231–234 (1977).
18. Figgins, J. & Morr, D. K. Defects in heavy-fermion materials: unveiling strong correlations in real space. *Phys. Rev. Lett.* **107**, 066401 (2011).
19. Toldin, F. P., Figgins, J., Kirchner, S. & Morr, D. K. Disorder and quasiparticle interference in heavy-fermion materials. *Phys. Rev. B* **88**, 081101 (2013).
20. Zhu, J.-X., Julien, J.-P., Dubi, Y. & Balatsky, A. V. Local electronic structure and fano interference in tunneling into a Kondo hole system. *Phys. Rev. Lett.* **108**, 186401 (2012).
21. Hamidian, M. H. *et al.* How Kondo-holes create intense nanoscale heavy-fermion hybridization disorder. *Proc. Natl. Acad. Sci. USA* **108**, 18233–18237 (2011).

22. Clerc, J., Giraud, G., Laugier, J. & Luck, J. The electrical conductivity of binary disordered systems, percolation clusters, fractals and related models. *Adv. Phys.* **39**, 191–309 (1990).

Acknowledgements

This work was supported by the National Natural Science Foundation of China (NSFC Grant No. 11522435), the State Key Development Program for Basic Research of China (Grant No. 2015CB921303), the Strategic Priority Research Program (B) of the Chinese Academy of Sciences (Grant No. XDB07020200) and the Youth Innovation Promotion Association CAS.

Author contributions statement

Y.Y. conceived the idea. Y.Y. and L.W. performed the research and wrote the paper.

Additional information

Competing financial interests: The authors declare no competing financial interests.

Supplementary Materials

Here we provide further analysis on the finite size effect and the critical scaling behavior of the dc conductivity.

Figure S1 compares the difference in the dc conductivity, $\sigma_{dc}(\beta t = 8) - \sigma_{dc}(\beta t = 4)$, for $L = 6, 8, 10, 12$. We see that the critical doping is almost unchanged with increasing lattice size L . We note that the extrapolation at $x = 0.99$ cannot be trusted as the doping is actually $(L^2 - 1)/L^2$, which varies with L . Similar variations exist for other doping, but are less crucial.

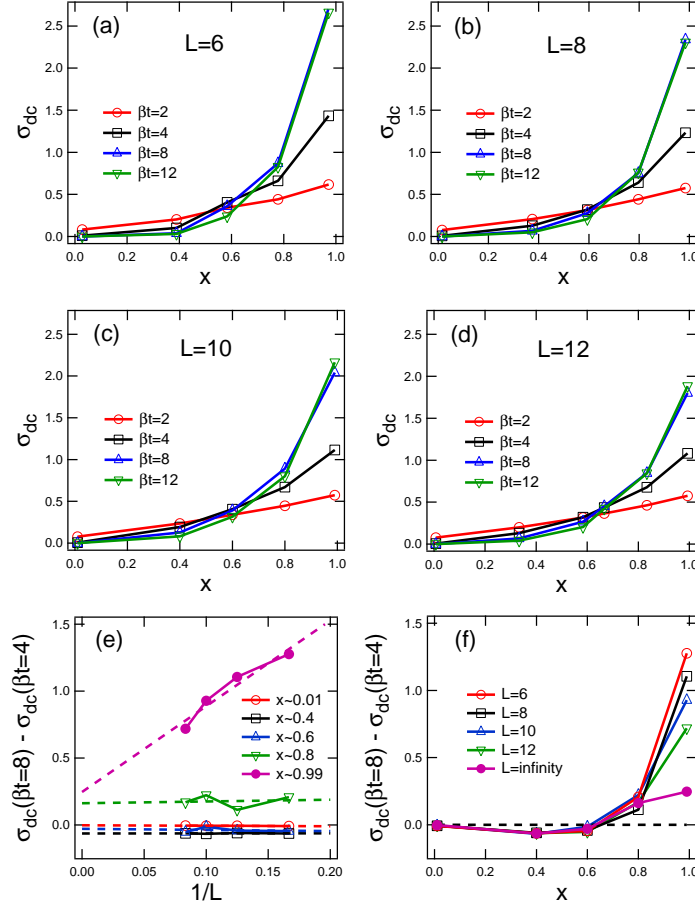


Figure S1. Lattice size dependence of the dc conductivity σ_{dc} . (a-d) σ_{dc} as a function of doping x at different temperatures for the lattice size $L = 6, 8, 10$, and 12 . (e) $\sigma_{dc}(\beta t = 8) - \sigma_{dc}(\beta t = 4)$ as a function of L for different dopings, showing the size dependence of the metallic or insulating behavior. The dashed lines illustrate linear extrapolations to the numerical data. (f) Doping dependence of $\sigma_{dc}(\beta t = 8) - \sigma_{dc}(\beta t = 4)$ for different lattice sizes, showing slight change in the critical doping $x_c \approx 0.6$ for the insulator-to-metal transition.

Figure S2 shows a power law fit to the dc conductivity, $\sigma_{dc} - \sigma_{dc}(x_c)$, with $(x - x_c)^\mu$ for $L = 12$ and $\beta t = 12, 14$ and 16 . The fit yields $\mu = 1.67, 1.56$ and 1.44 , respectively, while previous theories have predicted $\mu \approx 1.3$ for zero temperature and 2D infinite lattice. Our results are close to the predicted values.

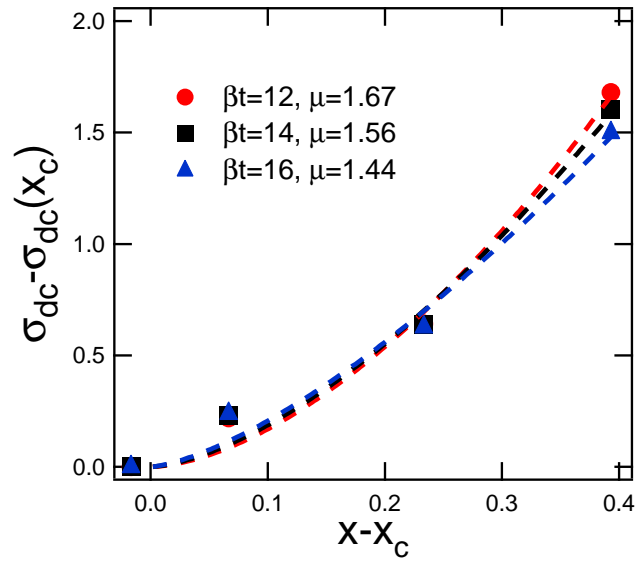


Figure S2. Fit to the dc conductivity, $\sigma_{dc} - \sigma_{dc}(x_c)$, with $(x - x_c)^\mu$ for $L = 12$ and $\beta t = 12, 14$ and 16 .